Local strain approaches for LCF life prediction of ship welded joints

Pasqualino CORIGLIANO [a,1], Vincenzo CRUPI[a], Pingsha DONG[b], Wolfgang FRICKE[b], Eugenio GUGLIELMINO[a]

[a] *Department of Engineering, University of Messina: pcorigliano@unime.it, crupi.vincenzo@unime.it, eguglie@unime.it*
[b] *Department of Naval Architecture and Marine Engineering, University of Michigan, Ann Arbor, MI 48105, United States: dongp@umich.edu*
[c] *Hamburg University of Technology. Institute for Ship Structural Design and Analysis: w.fricke@tu-harburg.de*

Abstract. The aim of this research activity is to predict the low-cycle fatigue life of welded joints used for ship structures, applying two methods: the effective notch strain approach and the structural strain approach. The first method was applied performing elastic-plastic finite element analyses (FEA), using different cyclic stress-strain curves for base material, heat affected zone and weld metal, while the second method is mesh insensitive for applications in high cycle fatigue regime and has recently been adapted for applications in low cycle fatigue regime. The geometry used for the first method was acquired by means of a 3D scanner. Effective notch strain results and structural strain results were used to predict the low cycle fatigue life.

Keywords. Low-cycle fatigue; welded joints; ship structures; structural strain method; finite element analysis; fatigue life prediction.

1. Introduction

Fractures in ship structures are frequently due to fatigue. Most ship structures consist of plate details, connected to longitudinal and transverse members by welded joints, which are the sites of high stress concentrations, and are subject to severe environmental loading from wave pressure, ship motions and loading/unloading operations, which induce significant fatigue loads. The presence of stress concentrations and fatigue loads leads to cyclic stress that exceeds the yield stress locally and some cracks, related to low-cycle fatigue (LCF), can be detected in ship structures within a few years of their service life.
The literature on the approaches for fatigue strength assessment of welded joints was reviewed by Fricke [1]. The most common approaches include: nominal stress approach (the simplest and most frequently used), structural hot-spot stress approach [2, 3, 4], effective notch stress approach using the fictitious notch radius [5, 6], notch stress intensity factor approach [7, 8], critical distance methods [9, 10, 11], thermographic

[1] Pasqualino Corigliano, Corresponding author, Department of Engineering, University of Messina,: Contrada di Dio - 98166 - Sant'Agata, Messina, Italy. pcorigliano@unime.it.

method [11, 12, 13, 14], notch strain approach [15], crack propagation approach [16], and the structural strain method [17].
In a previous study [18], full-field techniques (Digital Image Correlation DIC and infrared thermography IRT) were applied during LCF tests, carried out on T-welded joint and a specific procedure was developed to analyze the response of the investigated welded joint under LCF loading. Some of the authors have already applied full-field techniques for the assessment of different materials used for marine structures: structural steel [19, 20] under static and fatigue loading, Iroko wood under static loading [21] and explosive welded joints [22].
The aim of the present study is the further development of the proposed procedure in order to predict the LCF life of the same welded joints using the effective notch strain approach and the structural strain approach.

2. Low-cycle fatigue tests

The investigated specimen is made of mild steel S235JR, being widely applied in shipbuilding. Welding was performed using the MAG process with 1.2 mm thick wire acc. to DIN ISO 14341-A-G4Si1. The small-scale specimens were produced in order to recreate the loading and boundary conditions, as shown in figure 1, of the full-scale model, realized at the Hamburg University of Technology.
Table 1 reports the parameters and the results of the tests [18]: test frequency (f), applied displacement amplitude (u_a) at the grips and the experimental number of cycles to failure (N_{f_exp}).

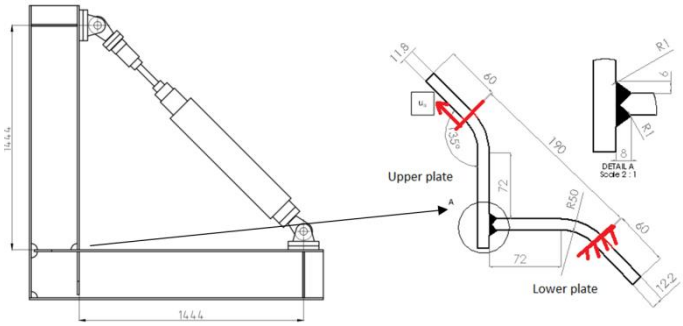

Figure 1. Full-scale and small-scale specimen.

Table 1. Parameters and results of LCF tests [18].

Test	Displacement amplitude u_a[mm]	Test frequency f [Hz]	Cycles to failure N_{f_exp}
1	2.5	0.1	375
2	2.5	0.1	430
3	2	1	620
4	2	1	628
5	2	0.1	510
6	1.5	1	1028
7	1.5	1	2312
8	1	1	5000
9	1	1	8400

3. Nonlinear FE analysis

Three 3D FE models of the welded joints were realized by means of ANSYS software. A nonlinear analysis was performed considering a multilinear kinematic hardening. The mesh was realized using 20-nodes solid elements and refined according to the IIW recommendation [23]. A specific procedure was developed in a previous study of the authors [18] to analyze the response of the investigated welded joint under LCF loading. It is based on the following steps: the assessment of the cyclic stress–strain curves of the different zones (BM, HAZ, and WM), depending on hardness values, the realization of a nonlinear FEA considering the different material properties, and the validation of FE model by means of the experimental data, obtained by DIC technique. The different cyclic curves used for the FE analyses are shown in figure 2. More information about the hardness measurements and the evaluation of the cyclic mechanical properties of the three zones are reported in [18].

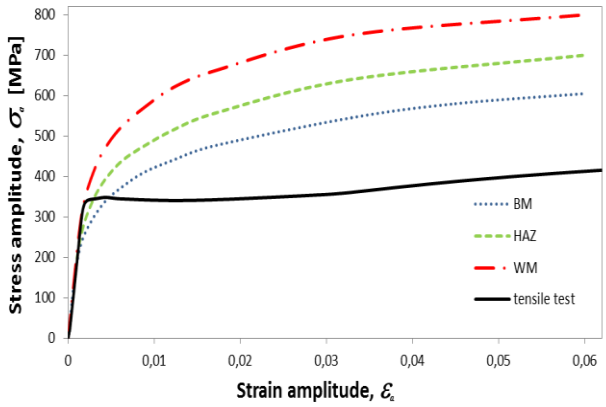

Figure 2. Cyclic stress–strain curves of the different material zones (BM, HAZ, WM).

In the present study, the proposed procedure was further developed in order to predict the fatigue life and to obtain the 3D model from scan measurements. Nominal values of the geometry were used in a first FE model (model 1): the width of the two plates is 40 mm, the thicknesses are 12 mm for the two plates, and the weld toe radius is 1 mm. The strain pattern, detected by means of DIC technique, showed a marked asymmetry of the two plates [18], while model 1 showed a general symmetry. From the measurement of the specimen, the width of the two plates was found 40 mm, while the thickness was found to differ from the nominal value of 12 mm: 11.8 mm for the upper plate and 12.2 mm for the lower plate. For this reason, model 1 was discarded for the FEA and, a second model (model 2) was made taking into account the different thicknesses of the plates, so a better agreement with respect to the experimental strains, detected by means of DIC technique [18], was achieved.

A third FE model (model 3) was considered, with a geometry acquired by means of 3D scan measurements, in order to take into account further parameters such as thicknesses along the plate, real curvature of the plates and possible misalignment of the plates in addition to the bending process. As GOM 3D scanner was used in order to measure the exact geometry of the specimen. The ATOS system allows acquiring the point clouds of the external surfaces and a surface mesh of the entire specimen, which

needs to be used by a commercial CAD program in order to create surface and solid model. Thus, surfaces and solid model were achieved with a commercial CAD program.

The solid model was imported into ANSYS software, the mesh refinement was made in accordance with IIW recommendations [23] and the properties of the different materials zones (BM, HAZ, WM) were inserted as done for all analyses. The toe radius was fixed equal to 1 mm also for model 3 in order to make a comparison with model 2. The results, in terms of first principal strain at the max load value, for an applied displacement of 2.5 mm, are shown in figure 3.

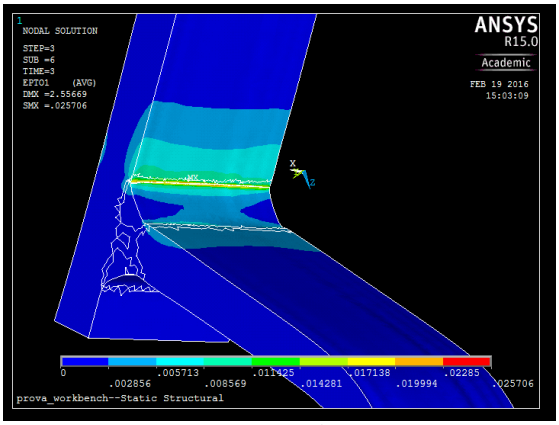

Figure 3. First principal strain of model 3 at max load value.

4. Low-cycle fatigue life prediction using the effective notch strain approach

If the load is applied to model 3 in order to compute the effective notch strain, attention should be paid to the value of the toe radius, otherwise wrong predictions could be achieved. Sometimes it is possible to find in reality small radii of 0.2 - 0.3 mm with very high local stresses and strains, but these are less effective due to the microstructural-support effects. Thus, if the effective notch strain is evaluated according to the real geometry, the real notch radius should be replaced with the fixed radius of 1 mm. For this reason the effective notch strain is calculated for both, model 2 and model 3, with the fixed radius of 1 mm in order to make a comparison and to analyze the effects due to real geometry on the LCF life.

The LCF prediction is based on the proposal by Saiprasertkit et al. [15] using the effective strain range in the weld toe rounded by a fixed radius of 1 mm, similar as in the effective notch stress approach for the high-cycle fatigue regime. A $\Delta\varepsilon$ - N curve could be obtained, when using the fixed radius, being in good agreement with LCF tests.

As the notch is characterized by a multiaxial strain state, the effective notch strain range $\Delta\varepsilon_{eff}$ has been determined. This is calculated in accordance with Saiprasertkit et al. [15] as the sum of the elastic and plastic part:

$$\Delta\varepsilon_{eff} = \Delta\bar{\varepsilon_t} = \frac{\Delta\bar{\sigma}}{E} + \Delta\bar{\varepsilon_p} \quad (1)$$

$$\Delta\bar{\sigma} = \sqrt{\frac{1}{2}\left[(\Delta\sigma_x - \Delta\sigma_x)^2 + \left(\Delta\sigma_y - \Delta\sigma_z\right)^2 + (\Delta\sigma_z - \Delta\sigma_x)^2 + 6\left(\Delta\tau_{xy}{}^2 + \Delta\tau_{yz}{}^2 + \Delta\tau_{zx}{}^2\right)\right]} \quad (2)$$

$$\Delta\bar{\varepsilon_p} = \frac{1}{3}\sqrt{2\left[\left(\Delta\varepsilon_{p,x} - \Delta\varepsilon_{p,y}\right)^2 + \left(\Delta\varepsilon_{p,y} - \Delta\varepsilon_{p,z}\right)^2 + \left(\Delta\varepsilon_{p,z} - \Delta\varepsilon_{p,x}\right)^2 + \frac{3}{2}\left(\Delta\gamma_{p,xy}{}^2 + \Delta\gamma_{p,yz}{}^2 + \Delta\gamma_{p,zx}{}^2\right)\right]} \quad (3)$$

The effective notch strain range results $\Delta\varepsilon_{eff}$ obtained from the FE analyses and the numbers of cycles to failure N_{f_exp} in the experimental tests are shown in Table 2. The crack initiation life N_i in Table 2 is assumed to be the 80% of the number of cycles to failure, which corresponds to the observed 20% maximum load drop, due to early crack propagation.

Table 2. Effective notch strain $\Delta\varepsilon_{eff}$, numbers of cycles to failure N_{f_exp}, crack initiation life N_i.

Model 2 $\Delta\varepsilon_{eff}$ %	**Model 3** $\Delta\varepsilon_{eff}$ %	N_{f_exp}	N_i
3.10	3.24	375	300
		430	344
2.38	2.43	620	496
		628	502
		510	408
1.67	1.63	1028	822
		2312	1849
1.07	0.88	5000	4000
		8400	6720

Figure 4 reports the $\Delta\varepsilon_{eff}$–N_i mean curve obtained by Saiprasertkit et al. [15], who analyzed a similar steel, and the results of the present investigation (model 3) with the mean regression line.

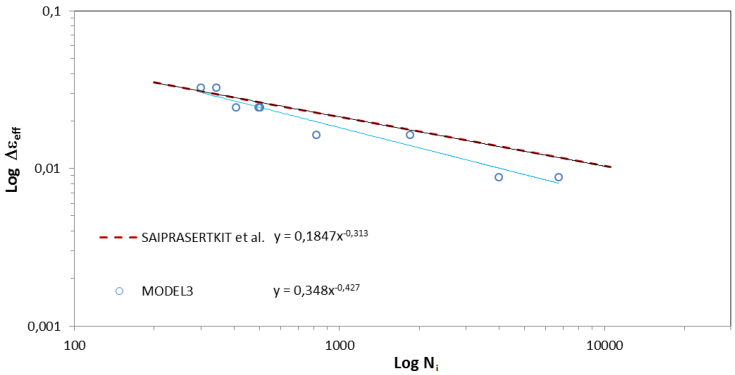

Figure 4. $\Delta\varepsilon_{eff}$–N_i curve obtained by Saiprasertkit et al. and by the present investigation.

5. Low-cycle fatigue life prediction using the Structural strain approach

Both traction based structural stress and structural strain methods are specifically developed for treatment of low cycle fatigue behavior in welded components in which

notch radii at weld locations such as weld toe are ill-defined [3, 17, 24-27]. The structural method is strictly consistent with the mesh-insensitive traction structural stress method [3, 24, 25] in which membrane and bending forms of traction stress components are calculated using nodal forces/moments from FEA output, if plastic deformation becomes negligible. This is because both methods are formulated based on the fundamental assumption that material points on a through-thickness cut plane remain on the same plane during deformation, but the plane may rotate and/or translate in space, i.e., "plane-remaining-plane" for short. When dealing with elastic deformation in high cycle fatigue regime, the mesh-insensitive traction structural stress method [25] extracts through-thickness membrane and bending parts of a traction stress component (note: a total of three traction components are available), which can be related to structural strain by Hooke's law [17, 26, 27]. When dealing elastic-plastic deformation in low cycle fatigue regime, there are two major methods [17, 26, 27] that can be used for computing structural strain. One is by correcting elastically calculated traction structural stresses by imposing both yield and equilibrium conditions [17] and the other is to compute equivalent linear strain distribution from nonlinear finite element results in which cyclic stress-strain relation is used [25]. The latter method is used here since stress-strain curves for base metal (BM), weld metal (WM), and heat affected zone (HAZ) were available from an early study. A two dimensional (2D) plane-strain finite element model is used here for calculating structural strain parameter under displacement controlled loading conditions, as illustrated in Figure 5. Note that in performing structural strain calculations, there is no need to introduce an artificial weld radius in the finite element model, as shown in Figure 5. Among both hypothetical cracking planes A-A and B-B, it was found that plane A-A is much more critical since its structural strain is about 30% higher along A-A than that along B-B. Therefore, structural strain calculations along A-A will be considered hereafter.

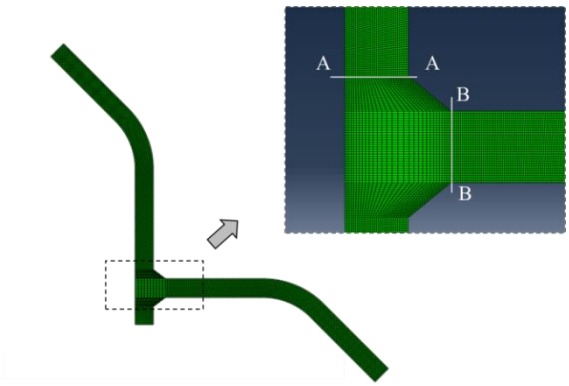

Figure 5. FE model and hypothetical crack planes (A-A and B-B) for structural strain calculations.

Based on an earlier study by some of the authors [18] of this paper, cyclic stress-strain curves are available for BM, WM, and HAZ regions, shown in Figure 2, which are also given in Figure 6. These regions are mapped onto the same regions in the FE model in Figure 5 and assigned with their respective stress-strain curves.

As a demonstration on how structural strain is calculated, consider the load case with displacement amplitude of u_a=1mm. The local strain (i.e., ε_y, normal to A-A) results obtained from nonlinear FE analysis (using commercial code ABAQUS) along

A-A are shown as the dashed lines in Figure 7, in which highest strain value occurring weld toe. The structural strain normal to A-A according definitions given in [17] can then be calculated as:

$$\varepsilon_m = \frac{1}{t} \cdot \int_{-t/2}^{t/2} \varepsilon_y(x) dx$$
$$\varepsilon_b = \frac{6}{t^2} \int_{-t/2}^{t/2} \varepsilon_y(x) x dy \quad (4)$$

The resulting structural strain distribution is shown as the solid line in Figure 7, with a negligible membrane strain. The peak structural value occurs at x=0, which can be converted to structural strain range by multiplying a factor 2 for fatigue test data interpretation purpose, since applied load ratio (R) in terms of displacement is R=-1. Note that the results shown in Figure 7 is based on base metal (BM) stress-strain curve applied to the entire model, which serves as a case for comparison with the results when BM, WM, and HAZ stress-strain curves are used, to be discussed next. For all four displacement controlled loading conditions, the structural strain range results summarized in Figure 8, labeled as "using BM stress-strain curve only".

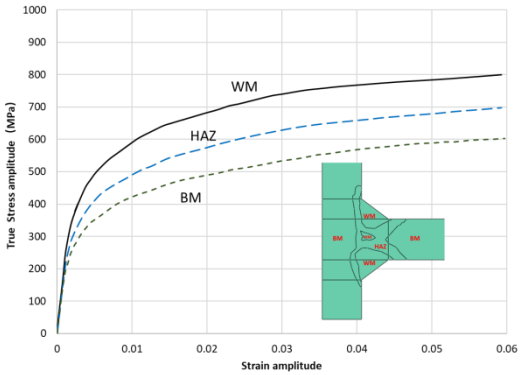

Figure 6. Cyclic material properties.

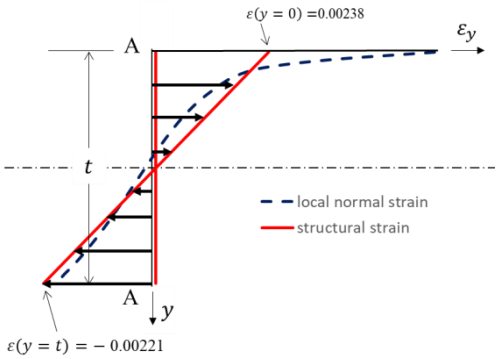

Figure 7. Structural strain versus local strain distribution.

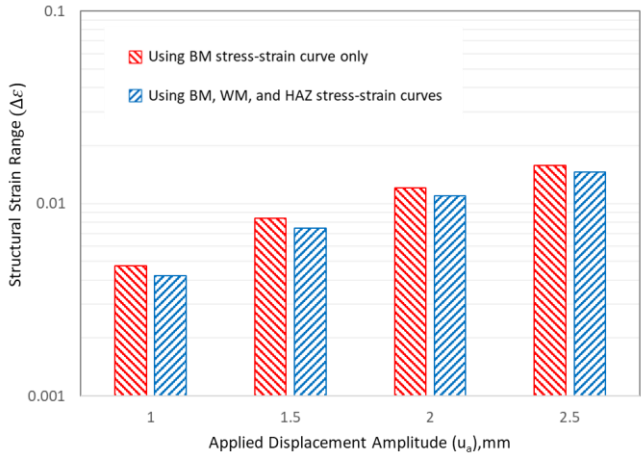

Figure 8. Structural strain range results corresponding to LCF fatigue test conditions.

With the same FE analysis and structural strain calculation procedures, the structural strain ranges for the four loading conditions by considering BM, WM, and HAZ stress-strain curves (see Figure 6) are also shown in Figure 8, labeled as "using BM, WM, and HAZ stress-strain curves". Note that log scale is used for the ordinate in Figure 8 since the fatigue test data are typically presented in log-log scale. Although the use of "BM stress-strain curve only" tends to over predict the structural strain values somewhat, the difference between two sets of the structural strain results is insignificant. This is further demonstrated by plotting the fatigue test data in terms of equivalent structural strain range parameter, defined as [17, 24-27]:

$$\Delta \mathrm{E}_s = \frac{\Delta\varepsilon}{t^{\frac{2-m}{m}} I(r)^{\frac{1}{m}}} \tag{5}$$

where,

$$I(r)^{\frac{1}{m}} = 2.1549 \cdot r^6 - 5.0422 \cdot r^5 + 4.8002 \cdot r^4 - 2.0694 \cdot r^3 + 0.561 \cdot r^2 + 0.0097 \cdot r + 1.5426 \tag{6}$$

which is directly taken from [25] for applications under displacement controlled fatigue conditions. The low-cycle fatigue test data can then be compared with ASME Div 2 master S-N curve representing over 1000 large scale fatigue tests (large scale is defined when the ratio width to thickness W/t>=10 in ref. [25]), with cycle to failure ranging from 10^2 to 10^8 (see lines in Figure 9). The structural strain calculation using elastic correction or nonlinear FEA methods, as Master S-N curve, implies through-thickness failure criterion. It is worth noting that overall correlation between the new test data and ASME master S-N curve scatter is rather reasonable, particularly when BM, WM, and HAZ stress-strain curves were used in computing structural strains. Figure 9 also

suggests if WM and HAZ stress-strain curves are not available, the use of BM stress-strain curve can still yield acceptable results, as shown by the solid symbols.

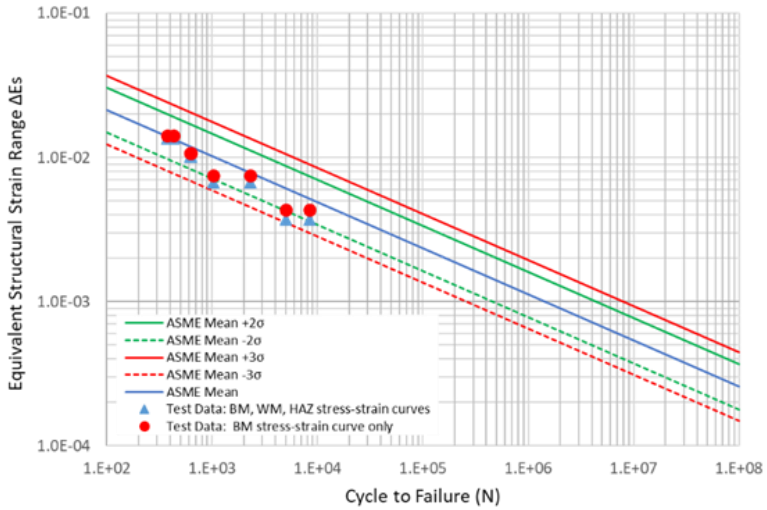

Figure 9. Comparison of the new LCF fatigue test data with ASME Div Master S-N curve scatter band in terms of equivalent structural strain range.

Conclusions

A procedure for the construction of a FE model of a fillet welded joint by means of a 3D scanner was applied in order to take into account parameters such as: thicknesses along the plate, real curvature of the plates and possible misalignment of the plates after the bending process.

The local geometry might govern the LCF behaviour, as was the case due to plate thickness differences by only 0.4 mm, the effective notch strain method works quite well also in this case for the prediction of LCF life.

Applying the structural strain approach, the low-cycle fatigue test data can be compared with ASME Div 2 master S-N curve representing over 1000 large scale fatigue tests with cycle to failure ranging from 10^2 to 10^8. The structural strain method works very well with the test data. If the different material properties are not available, the base material properties can still be used for the structural strain calculation.

References

[1] W. Fricke. Recent Developments and Future Challenges in Fatigue Strength Assessment of Welded Joints, *P I MechEng C-J Mech* **229** (2015), 1234-1249.

[2] D. Radaj, C.M. Sonsino, W. Fricke, Recent developments in concepts of fatigue assessment of welded joints, *Int J Fatigue* **31**(2009), 2-11.

[3] P. Dong, A structural stress definition and numerical implementation for fatigue analyses. Int J Fatigue **23** (2001), 865-876.

[4] W. Fricke, A. Kahl, Comparison of different structural stress approaches for fatigue assessment of welded ship structures,. *Mar Struct* **18** (2005), 473-488.
[5] D. Radaj, C.M., Sonsino, W. Fricke, *Fatigue Assessment of Welded Joints by Local Approaches*. Cambridge, Woodhead Publ Series in Welding and Other Joining Technologies.
[6] C.M. Sonsino, D. Radaj, U. Brandt, H.P. Lehrke, Fatigue assessment of welded joints in AlMg 4.5 Mn aluminium alloy (AA 5083) by local approaches, I*nt J Fatigue* **21** (1999), 985-99.
[7] P. Lazzarin, R. Tovo, A notch intensity factor approach to the stress intensity of welds, *Fatigue Fract Eng Mater Struct* **21** (1998), 1089-1103.
[8] B. Atzori,P. Lazzarin, G. Meneghetti,M. Ricotta, Fatigue design of complex welded structures, *Int J Fatigue* **31 (**2009), 59-69.
[9] D. Taylor, N. Barrett, G. Lucano, Some new methods for predicting fatigue in welded joints, *Int J Fatigue* **24** (2002), 509-518.
[10] D. Taylor, *The theory of critical distances: a new perspective in fracture mechanics*, Oxford, UK. Elsevier, 2007.
[11] V. Crupi, E. Guglielmino, A. Risitano,D. Taylor, Different methods for fatigue assessment of T welded joints used in ship structures, *J. Ship Res* **51**(2007), 150-159.
[12] J.L. Fan, X.L. Guo, C.W. Wu, Y.G. Zhao, Research on fatigue behavior evaluation and fatigue fracture mechanisms of cruciform welded joints, *Mater. Sci. Eng. A* **528** (2011), 8417-8427.
[13] P. Williams, M. Liakat, M.M. Khonsari, O.M. Kabir, A thermographic method for remaining fatigue life prediction of welded joints, *Materials and Design* **51** (2013), 916-923.
[14] V. Crupi, E. Guglielmino, M. Maestro, A. Marinò, Fatigue analysis of butt welded AH36 steel joints, Thermographic Method and design S-N curve, *Mar Struct* **22** (2009), 373-386.
[15] K. Saiprasertkit, T. Hanji, C. Miki, Fatigue strength assessment of load carrying cruciform joints in low and high cycle fatigue region based on effective notch stress approach, *Int J Fatigue* **40** (2012), 120-128.
[16] M.D. Chapetti, L.F. Jaureguizahar, Fatigue behavior prediction of welded joints by using an integrated fracture mechanics approach, *Int J Fatigue* **43** (2012), 43-53.
[17] P. Dong, X. Pei, S. Xing, M. H. Kim, A structural strain method for low-cycle fatigue evaluation of welded components, *International Journal of Pressure Vessels and Piping*, **119** (2014), 39-51.
[18] P. Corigliano, V. Crupi,W. Fricke, N. Friedrich, E. Guglielmino, Experimental and numerical analysis of fillet-welded joints under low-cycle fatigue loading by means of full-field techniques, *P I MechEng C-J Mech* **229** (2015), 1327-1338. https://doi.org/10.1177/0954406215571462.
[19] P. Corigliano, V. Crupi, G. Epasto, E. Guglielmino, G. Risitano, Fatigue assessment by thermal analysis during tensile tests on steel, *Procedia Eng* **109** (2015), 210–218.
[20] P. Corigliano, G. Epasto, E. Guglielmino, G. Risitano, Fatigue analysis of marine welded joints by means of DIC and IR images during static and fatigue tests, *Eng. Fract. Mech* **183** (2017), 26–38. doi:10.1016/j.engfracmech.2017.06.012.
[21] V. Bucci, P. Corigliano, V. Crupi, G. Epasto, E. Guglielmino, A. Marinò, Experimental investigation on Iroko wood used in shipbuilding, *P. I. Mech. Eng. C-J. Mec* **231**(2017), 128–139.
[22] P. Corigliano, V. Crupi, E. Guglielmino, A.M Sili, Full-field analysis of AL/FE explosive welded joints for shipbuilding applications, *Mar Struct* **57** (2018), 207-218. doi:10.1016/j.marstruc.2017.10.004.
[23] *Fatigue design of welded joints and components*, International Institute of Welding. Cambridge, Abington Publishing, Abington, 1996.
[24] P. Dong, A robust structural stress method for fatigue analysis of offshore/marine structures, *Journal of offshore mechanics and Arctic engineering* **127** (2005), 68-74.
[25] P. Dong, J.K. Hong, D.A. Osage, D.J. Dewees, M. Prager, *The master SN curve method: an implementation for fatigue evaluation of welded components in the ASME B&PV CODE, Section VIII, Division 2 and API579-1/ASME FFS-1*, Welding Research Council Bulletin, 2010.
[26] X. Pei, W. Wang, P. Dong, An Analytical-Based Structural Strain Method for Low Cycle Fatigue Evaluation of Girth-Welded Pipes. *ASME 2017 Pressure Vessels and Piping Conference (pp. V03BT03A015-V03BT03A015), American Society of Mechanical Engineer* (2017).
[27] D. A. Osage, P. Dong, D. Spring, Fatigue assessment of welded joints in API 579-1/ASME FFS-1 2016-existing methods and new developments, *Procedia Engineering* **213** (2018), 497-538.